NeuroImage 59 (2012) 1239–1248

Contents lists available at SciVerse ScienceDirect

NeuroImage

journal homepage: www.elsevier.com/locate/ynimg

Convergence and divergence of thickness correlations with diffusion connections across the human cerebral cortex

Gaolang Gong [a,b], Yong He [a], Zhang J. Chen [b], Alan C. Evans [b,*]

[a] State Key Laboratory of Cognitive Neuroscience and Learning, Beijing Normal University, Beijing, China
[b] McConnell Brain Imaging Center, Montreal Neurological Institute, Montreal, QC, Canada

ARTICLE INFO

Article history:
Received 9 June 2011
Revised 4 August 2011
Accepted 8 August 2011
Available online 22 August 2011

Keywords:
Thickness correlation
Diffusion connectivity
Cerebral cortex
Cortical network
Magnetic resonance imaging

ABSTRACT

Cortical thickness correlation across individuals has been observed. So far, it remains unclear to what extent such a correlation in thickness is a reflection of underlying fiber connection. Here we explicitly compared the patterns of cortical thickness correlation and diffusion-based fiber connection across the entire cerebral cortex, in 95 normal adults. Interregional thickness correlations were extracted by using computational neuroanatomy algorithms based on structural MRI, and diffusion connections were detected by using diffusion probabilistic tractography. Approximately 35–40% of thickness correlations showed convergent diffusion connections across the cerebral cortex. Intriguingly, the observed convergences between thickness correlation and diffusion connection are mostly focused on the positive thickness correlations, while almost all of the negative correlations (>90%) did not have a matched diffusion connection, suggesting different mechanisms behind the positive and negative thickness correlations, the latter not being mediated by a direct fiber pathway. Furthermore, graph theoretic analysis reveals that the thickness correlation network has a more randomized overall topology, whereas the nodal characteristics of cortical regions in these two networks are statistically correlated. These findings indicate that thickness correlations partly reflect underlying fiber connections but they contains exclusive information, and therefore should not be simply taken as a proxy measure for fiber connections.

Introduction

The inter-subject variability of brain morphometric features has been quantitatively reported, using both neuroimaging and postmortem data (Li et al., 2010; Thompson et al., 1996; Zilles et al., 1997). Intriguingly, the morphometric variability across individuals is not uniquely present but shows similar patterns among various areas, suggesting a structural association/interaction of these areas in some aspect. For instance, Mechelli et al. (2005) have reported covariance of gray matter density between multiple bilateral homotopic regions across adult population. Also, our group demonstrated significant thickness correlations within the cerebral cortex (Lerch et al., 2006), e.g. between Broca's and Wernicke's area that are well-known as language-related areas. Particularly, further studies from our laboratory found altered patterns of interregional thickness correlation under abnormal brain conditions such as Alzheimer's disease (He et al., 2008) and multiple sclerosis (He et al., 2009).

So far, the biological mechanisms underlying the thickness correlation among cortical areas remain unclear. One speculation is that related areas covary morphometrically as a result of mutually trophic effects that are mediated by direct axonal connections (Ferrer et al., 1995; Mechelli et al., 2005). This hypothesis implies that cortical thickness correlation should reflect an underlying fiber connection between the two areas and therefore leads to the expectation of convergence between these two measures. There has been some evidence supporting this expectation. For instance, Lerch et al. (2006) showed that the pattern of thickness correlation for Brodmman area 44 is similar to the tractography map obtained from previous diffusion tensor imaging (DTI) studies. In addition, He et al. (2007) reported that the 15 regional pairs showing the most significant thickness correlations correspond with known white matter tracts according to previous neuroanatomy literature. However, the nature of relationship between thickness correlation and underlying anatomical connectivity has not yet been explicitly studied in the same population. In particular, while the convergence of thickness correlations with fiber connections has been demonstrated between specific regions-of-interest, it is not known if this convergence could be generalized across the entire cerebral cortex.

Once interregional thickness correlations are obtained for all possible regional pairs, the cerebral cortex could be characterized as a structural network in which each cortical area represents a network node and two nodes/areas are considered connected if they have significant correlations of thickness across individuals (He et al., 2007). Graph theoretical analysis on the thickness correlation network in

* Corresponding author at: McConnell Brain Imaging Centre, Montreal Neurological Institute, Montreal QC, Canada H3A 2B4. Fax: +1 514 398 8948.
E-mail address: alan@bic.mni.mcgill.ca (A.C. Evans).

1053-8119/$ – see front matter © 2011 Elsevier Inc. All rights reserved.
doi:10.1016/j.neuroimage.2011.08.017

healthy adults has revealed attractive topological properties such as small-worldness and modular structure (Chen et al., 2008; He et al., 2007). Further studies have demonstrated significant network alterations that are specific to different brain diseases such as Alzheimer's disease (He et al., 2008) and multiple sclerosis (He et al., 2009). Similarly, Bassett et al. (2008) reported topological changes of gray matter volume correlation network in schizophrenia patients, as compared to normal controls. Meanwhile, the topology of human brain diffusion networks has been investigated in-vivo, using diffusion MRI tractography (Hagmann et al., 2008; Iturria-Medina et al., 2008; Lo et al., 2010; Wen et al., 2011). Our group have developed a population-based cortical diffusion network using deterministic diffusion tractography (Gong et al., 2009b) and further extended it to allow for an individual-based cortical network using probabilistic tractography recently (Gong et al., 2009a). However, it remains unknown how the topology of the thickness correlation network is associated with the diffusion-based network.

In this study, we will systematically compare the patterns of cortical thickness correlation and diffusion connection across the entire cerebral cortex, which aims to clarify that whether cortical thickness correlation could be simply taken as a proxy observation of underlying fiber connections or it actually contains exclusive information representing an important aspect of interregional association/interaction not evident from diffusion MRI studies of fiber pathways.

Method

Subjects

The present study included data from 95 normal subjects (males, 47; females, 48; age, 19–85 years) (Gong et al., 2009a). All subjects were recruited for the International Consortium of Brain Mapping (ICBM) dataset at Montreal Neurological Institute (MNI) and have no history of neurological and psychiatric disorders. Our protocol was approved by the Research Ethics Committee of the Montreal Neurological Institute and Hospital. Informed consent was obtained from each subject.

MRI acquisition

All scans were performed on the same Siemens Sonata 1.5 T MRI scanner. Diffusion MRI was acquired by using a single-shot echo planar imaging-based sequence with sensitivity encoding and a parallel imaging factor of 2.0: coverage of the whole brain; 2.5 mm slice thickness with no inter-slice gap; 60 axial slices; repetition time (TR), 8000 ms; echo time (TE), 94 ms; 30 optimal nonlinear diffusion weighting directions with $b = 1000$ s/mm^2 and five additional images without diffusion weighting (i.e., $b = 0$ s/mm^2); average, 3; acquisition matrix, 96×96; field of view (FOV), 240×240 mm^2. Three-dimensional T1-weighted images with high resolution were obtained by a three dimensional gradient echo sequence with following parameters: 1 mm slice thickness with no interslice gap; 117 sagittal slices; TR, 22 ms; TE, 9.2 ms; flip angle, 30°; average, 1; acquisition matrix, 256×256; FOV, 256×256 mm^2.

Cortical parcellation

In this study, the automated anatomical labeling (AAL) template (Tzourio-Mazoyer et al., 2002) was used to parcellate the entire cerebral cortex into 78 cortical regions (39 for each hemisphere), each representing a node of the cortical network. For each subject, the parcellation was conducted in the MRI native space. Specifically, the T1-weighted image was first coregistered to the b0 image in the diffusion MRI space using a linear transformation. T1-weighted MR image was then nonlinearly mapped to the T1 template of ICBM152 in MNI space (Collins et al., 1994). The resulting transformation was inverted and further applied to warp the AAL mask from MNI space to the T1-weighted MRI and diffusion MRI native space in which the discrete labeling values were preserved by using a nearest-neighbor interpolation method. This parcellation procedure has been applied previously (Gong et al., 2009b). Specifically, the linear and nonlinear registrations were implemented using the MNI registration tool (Collins et al., 1994).

Regional cortical thickness correlation and network from structural MRI

The T1-weighted MR images were first registered into stereotaxic space, using a 9-parameter linear transformation. Images were corrected for non-uniformity artifacts using the N3 algorithm (Sled et al., 1998). The registered and corrected images were further segmented into gray matter, white matter, cerebrospinal fluid and background using a neural net classifier (Tohka et al., 2004; Zijdenbos et al., 2002). The inner and outer gray matter surfaces were then automatically extracted from each hemisphere using the CLASP algorithm (Kim et al., 2005; MacDonald et al., 2000). Cortical thickness was measured in native space using the linked distance (i.e. t-link) (Lerch and Evans, 2005) between the two surfaces at 40,962 vertices per hemisphere. The cortical thickness algorithm has been validated using both manual measurements (Kabani et al., 2001) and simulation approaches (Lee et al., 2006; Lerch and Evans, 2005). Using the generated AAL masks above, we divided the surface into 78 regions (Fig. 1a). For each subject, regional cortical thickness was defined as the average thickness of all vertices belonging to that region. A linear regression analysis was performed at every cortical region to remove the effects of multiple confounding variables: age, gender, and overall mean cortical thickness (He et al., 2007). The residuals of this regression were used to substitute for the raw cortical thickness values of each region. The Kolmogorov–Smirnov (KS) test on the residuals showed a p-value of 0.13, suggesting a normal distribution. The inter-regional symmetric correlation matrix R_{ij} (78×78) was then constructed by calculating the Pearson correlation coefficients across the 95 individuals between the cortical thicknesses of every regional pair. To estimate the variance of this matrix across different sampling populations, we generated 1000 bootstrap samples (95 subjects for each sample) by resampling with replacement from our 95 individuals (Efron and Tibshirani, 1993) and then computed the thickness correlation matrix for each bootstrap sample, using the same processing pipeline.

Regional diffusion connection and network from diffusion tractography

The estimation of regional diffusion-based anatomical connectivity using probabilistic tractography has been previously described (Gong et al., 2009a). Briefly, the diffusion-weighted images were first coregistered to a reference volume (i.e., the b0 image) using an affine transformation for the correction of head motion and eddy current-induced image distortion. Secondly, the local probability distribution of fiber direction was estimated at each voxel (Behrens et al., 2003a,b). Probabilistic tractography was then applied with a computation model allowing for automatic estimation of two fiber directions within each voxel. The connectivity probability from the seed region i to another region j was then defined by the number of fibers passing through region j divided by the total number of fibers sampled from region i (Behrens et al., 2007). Each AAL cortical region in turn was selected as the seed region and its connectivity probability to each of the other 77 regions was estimated. Notably, the probability from region i to j is not necessarily equivalent to the one from j to i because of the tractography dependence on the seeding location. However, these two probabilities are highly correlated across the cerebral cortex for all subjects (the least Pearson $R = 0.70$, $p = 10^{-50}$). Thus, we defined the undirectional connectivity probability between region i and j by averaging these two probabilities. Taken together, one 78×78 symmetric cortical diffusion network was yielded for

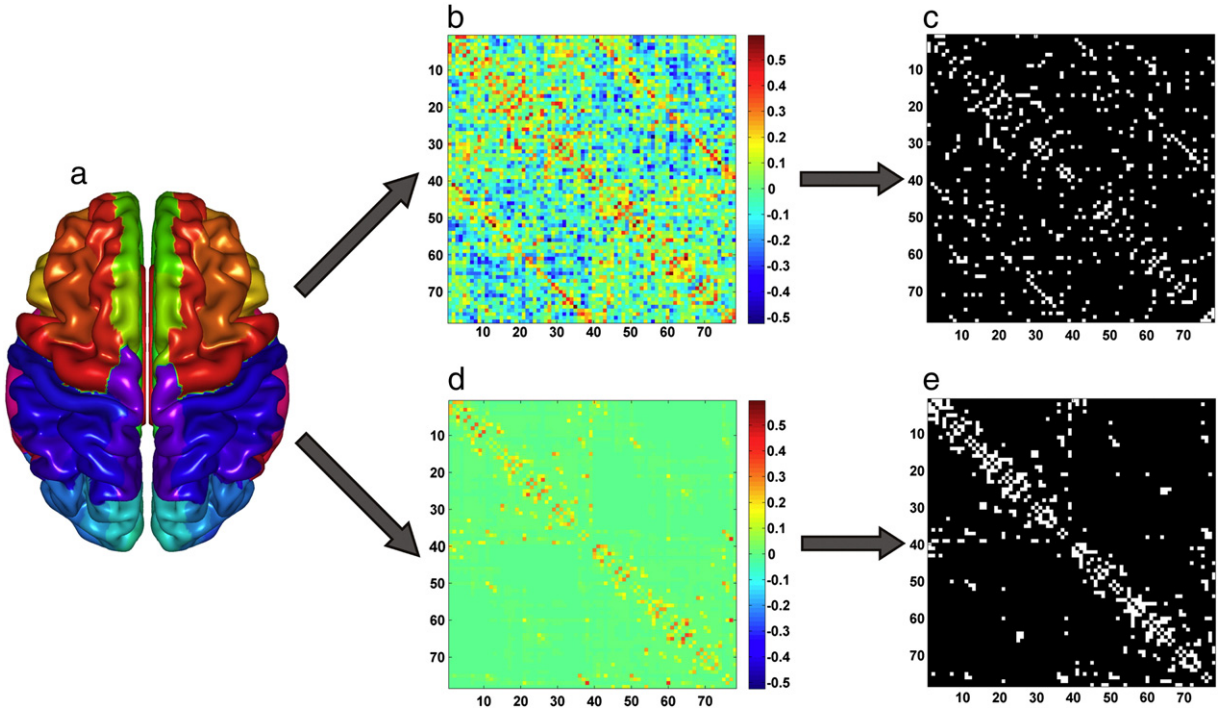

Fig. 1. The schematic processing for constructing both thickness correlation and diffusion networks. (a) The AAL template masks on the cortical surface. Each color represents one cortical region (78 in total); (b) The matrix of Pearson correlation coefficient in regional cortical thickness across the 95 individual, after factoring out the age, gender and mean cortical thickness; (c) The binarized matrix of thickness correlation using sparsity-based thresholding approach; (d) The population-averaged probability matrix of diffusion connections derived from diffusion MRI tractography; (e) The binarized matrix of diffusion connection after thresholding with the same sparsity value of (c). The order of cortical regions in the matrices is consistent with our previous study (Gong et al., 2009a,b). For more details, please see Method.

each subject, representing the fiber connectivity organization of the entire cerebral cortex (Gong et al., 2009a). Since the thickness correlation map is derived from the whole population, we averaged the diffusion connectivity probability across the 95 individuals for each regional pair, leading to a representative diffusion matrix for the whole population. Notably, the diffusion connectivity probability of the individual networks is highly correlated with the group diffusion networks (the least Pearson $R = 0.93$, $p = 10^{-100}$). Also, the network topology of the group diffusion network nicely captures the patterns of individual networks (see Fig. 7). Unless otherwise specified, the diffusion network in this study refers to mean diffusion network across the population. Likewise, we also generated 1000 mean diffusion networks for the 1000 bootstrap samples that were described above. Notably, for each bootstrap sample, the thickness correlation and mean diffusion network were computed from the same set of subjects and therefore are comparable in pairs.

Comparison of thickness correlation and diffusion connectivity

The above procedures result in one 78×78 symmetric correlation matrix for cortical thickness and one 78×78 symmetric probability matrix for diffusion connectivity across the whole population. For conceptual simplicity, our present study will focus on a presence/absence pattern (i.e. binary pattern) of thickness correlations and diffusion connections. Similar to previous studies (Achard and Bullmore, 2007; Bassett et al., 2008; He et al., 2008), we here employed a sparsity-based thresholding approach, where the sparsity was defined as the ratio of the number of actual connections to the number of possible connections ($78 * (78-1)/2 = 3003$) within the network. For example, threshold of sparsity 10% will result in the set of connections ($3003 * 10\% \approx 300$) with highest absolute values in the entire network. Specifically, we applied the same sparsity threshold to both matrices, ensuring the same number of supra-threshold regional pairs for both modalities. Since there is no definitive choice for a single threshold, we identified a thresholding range yielding a fully connected cortical network with a small-world topology (i.e. sigma>1.2), as previously proposed by Bassett et al. (2008). Here, the sparsity range of 4.4%–56.5% and 8.9%–25.2% satisfy the criterion of "a fully connected network with a small-world topology" for the diffusion network and thickness correlation network, respectively. We therefore chose the overlapping range 8.9%–25.2% as the final sparsity range in the present study. Notably, the binarizing step for DN construction has naturally removed out the effects of aging and sex on the network topology, given the empirical assumption that the macroscopic pattern of fiber connections (although not the connection strengths) is largely fixed across the normal adult population.

We further defined the similarity metric (SM) of distribution between the two modalities as the ratio of the number of regional pairs that were in agreement by simultaneously showing presence or absence of a connection in both modalities (N_{agree}) to the number of all possible regional pairs (N_{total}):

$$SM = \frac{N_{agree}}{N_{total}}$$

Here, regional pairs with a thickness correlation connection or diffusion connection represent the ones surviving the threshold of the thickness correlation or diffusion connection at a selected network sparsity. Also, we computed the percentage of convergence (PC) by dividing the number of convergent regional pairs (N_{con}) by the number of all supra-threshold regional pairs (N_{supra}, identical for both modalities due to the same sparsity):

$$PC = \frac{N_{con}}{N_{supra}}$$

The SM and PC indices were analyzed as a function of sparsity. We found these two metrics are significantly correlated ($R = 0.5$,

$p = 10^{-7}$) across the sparsity range. In addition, two random binary matrices with the same sparsity were generated 1000 times to estimate the SM and PC that would be expected by chance. Finally, since thickness correlation could be positive or negative, we further subdivided these indices for positive or negative thickness correlations only.

Comparison of network topological properties

Previous studies have demonstrated the small-world topology of both diffusion and thickness correlation networks, characterized by highly efficient information transfer both locally and globally (Gong et al., 2009b; He et al., 2007; Iturria-Medina et al., 2008). The small-world topology was originally proposed by Watts and Strogatz (1998) by using two classic graph parameters: clustering coefficient (Luce and Perry, 1949) and characteristic path length (Dijkstra, 1959). This concept was then generalized by introducing network efficiency that has a number of conceptual and technical advantages (Achard and Bullmore, 2007; Latora and Marchiori, 2003). Conceptually, the local clustering C and characteristic path length L correspond to the local and global efficiency of the network, respectively. Specifically, the inverse of the harmonic mean of shortest path length (d_{ij}) between each pair of nodes within the network is defined as the network global efficiency E_{glob}:

$$E_{glob}(G) = \frac{1}{N(N-1)} \sum_{i \neq j \in G} \frac{1}{d_{ij}}$$

Furthermore, the local efficiency for each node could be calculated as the global efficiency of the neighborhood subgraph G_i of the node. Theoretically, the local efficiency represents how much the complex network is fault-tolerant, indicating how well the information is communicated within the neighbors of a given node when this node is removed. The local efficiencies across all nodes within the network are further averaged to estimate the network local efficiency E_{loc}:

$$E_{loc}(G) = \frac{1}{N} \sum_{i \in G} E_{glob}(G_i)$$

The regional efficiency (E_{reg}) for a given node is defined as the inverse of mean harmonic shortest path length between this node and all other nodes in the network (Achard and Bullmore, 2007):

$$E_{reg}(i) = \frac{1}{N-1} \sum_{i \neq j \in G} \frac{1}{d_{ij}}$$

Since each of these network metrics has been computed for a specific sparsity range, a summary network metric is necessary. Here, we estimated the integrals of each metric curve over the range of the sparsity (8.9%–25.2%) as the summary metric. Such integrated metrics mathematically correspond to the areas under the metric curve and have been applied in recent brain network studies (Bassett et al., 2008; Gong et al., 2009a; He et al., 2007, 2008).

Results

Convergence of thickness correlation with diffusion connection across the cerebral cortex

The SM and PC between cortical thickness correlation and diffusion connection across the entire cerebral cortex are specific to the choice of the sparsity threshold and therefore have been plotted as a function of sparsity (Fig. 2). In the present study, we computed SM and PC for each bootstrap sample. The resulting sampling sets (sample size = 1000) of SM and PC could be used to estimate statistics such as mean and standard deviation (STD) for SM and PC.

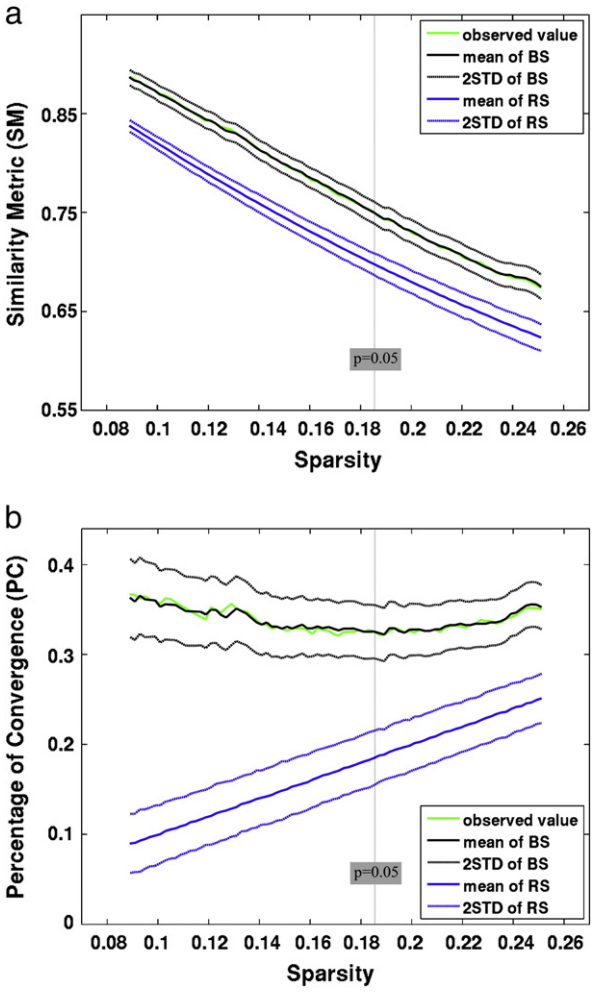

Fig. 2. The distribution similarity in between thickness correlation and diffusion connection. (a) Similarity metric (SM) as a function of sparsity; (b) Percentage of convergence (PC) as a function of sparsity. The statistics of SM and PC (mean and STD, black line) between thickness correlation and diffusion connection were estimated from the 1000 bootstrap samples (BS). The uncorrected $p = 0.05$ for the thickness correlation was marked out (i.e. sparsity of 18.6%). As shown, the observed values of SM and PC from the raw 95 subjects (green line) are very close to the mean of BS. The statistic of SM and PC (mean and STD, blue line) expected by chance were estimated from simulated 1000 random samples (RS). Clearly, the SM and PC are significantly higher than expected by chance over the entire range of sparsity.

Notably, the mean SM and PC of the bootstrap samples are very close to the SM and PC of the real 95 individuals over the entire range of sparsity, which is expected according to the bootstrapping theory (Efron and Tibshirani, 1993). Additionally, we calculated SM and PC for 1000 simulated pairs of random networks, representing the SM and PC values expected by chance. When more connections are present, a random network tends to be less agreed with another one (lower SM) but the percentage of convergence increases (higher PC), as shown in Fig. 2. Clearly, the SM and PC indices between thickness correlation and diffusion connection are significantly higher than expected by chance over the entire range of sparsity (two sample *t*-test, the maximum $p = 10^{-100}$ for SM, and $p = 10^{-100}$ for PC), indicating that thickness correlation and diffusion connection are not independently distributed across the cerebral cortex. However, only 35–40% of thickness correlations (Fig. 2b) have matched diffusion connections, which are compatible with poor rank correlation of weights between the two modalities across all regional pairs (Supplementary Fig. 1). These results suggest that a more complicated biological mechanism underlies thickness correlation across the entire cerebral cortex.

For deeper investigation, we examined the network at the lower limit of sparsity threshold (i.e. 8.9%). This lower limit of sparsity threshold results in the set of strongest/reliable thickness correlation or diffusion connection. The most reliable convergent regional pairs between these two modalities were visualized in Fig. 3, showing the majority of them are between ipsilateral or bilateral homotopic regions (Supplementary Table 2). Furthermore, these reliable convergences are between regions with a relatively short spatial distance.

Positive and negative thickness correlation across the cerebral cortex

Thickness correlations across the cerebral cortex have two directions: positive or negative (Fig. 4). As shown in Fig. 5a, there is no dramatic disproportion between positive and negative correlation over the entire sparsity range: approximately 40%–60% correlations are positive or negative depending on the sparsity. We further found that most negative correlations (around 80%) are between bilateral heterotopic (i.e. inter-hemispheric and inhomogeneous) regions, but positive correlations are mostly among ipsilateral (i.e. intra-hemispheric) or bilateral homotopic (i.e. inter-hemispheric and homogeneous) regions (Fig. 5b). Intriguingly, the convergence between thickness correlation and diffusion connection is largely confined to positive cortical correlations (Figs. 4 and 5c). About 60% of positive thickness correlations showed convergence with the diffusion connection over the sparsity range, whereas almost all (>90%) of the negative correlations were divergent with the diffusion connection. Such a dramatic contrast between positive and negative correlation suggests that different mechanisms underlie the positive and negative thickness correlation, the latter not being mediated by a direct fiber pathway.

Topological properties of the thickness correlation network (TCN) and diffusion network (DN)

The local and global efficiencies for both cortical networks as well as their matched random networks are calculated, as a function of the network sparsity. Specifically, 1000 matched random networks were generated at each sparsity using the random rewiring procedure described by Maslov and Sneppen (2002) that preserves the degree distribution. Compared with the matched random networks, both cortical networks showed a much higher local efficiency but similar global efficiency over the entire range of sparsity, indicating a small-world character for both cortical networks (Supplementary Fig. 2). As shown in Fig. 6, the TCN exhibited significantly higher global efficiency but much lower local efficiency than the DN over the range

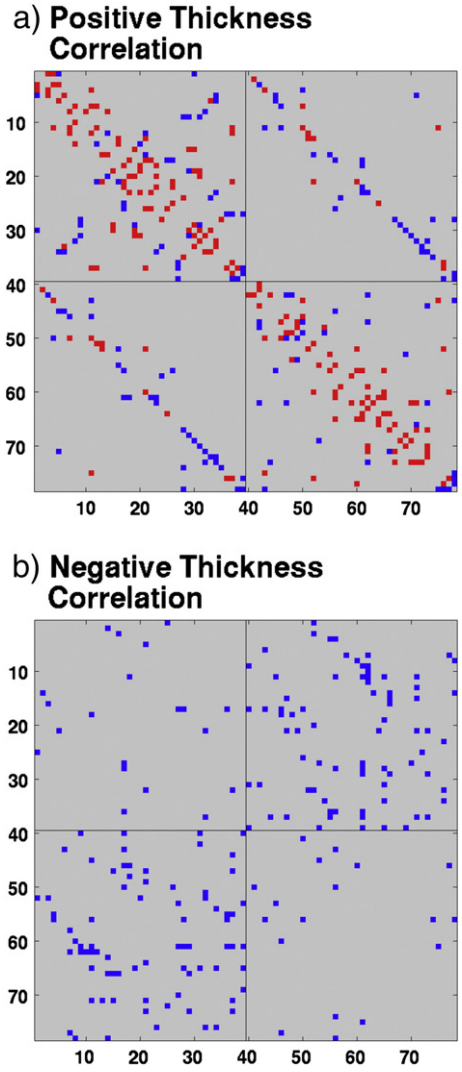

Fig. 4. Positive (a) and negative (b) thickness correlation matrix at the sparsity of 8.9%. In both (a) and (b), red or blue indicate the thickness correlation convergent or divergent with diffusion connection, respectively. Notably, the convergence between thickness correlation and diffusion connection appears only in the positive thickness correlations at this sparsity.

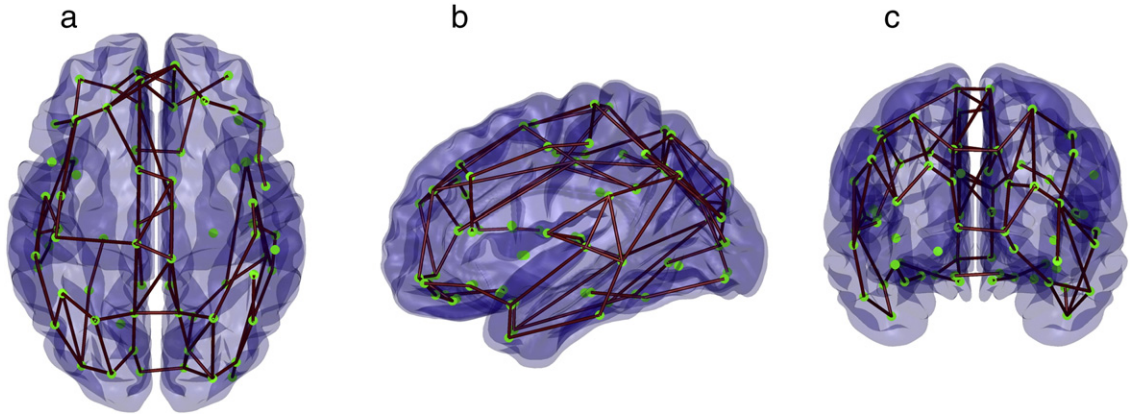

Fig. 3. The regional pairs showing reliable convergence between thickness correlation and diffusion connection (sparsity: 8.9%). Each green spot represents the center of an AAL region. The regional pairs with both thickness correlation and diffusion connection are linked by a red line. As shown, the majority of the convergence is between ipsilateral or bilateral homotopic regions that have relatively short distance. Importantly, all the regional pairs here are positively correlated in thickness, according to Fig. 4.

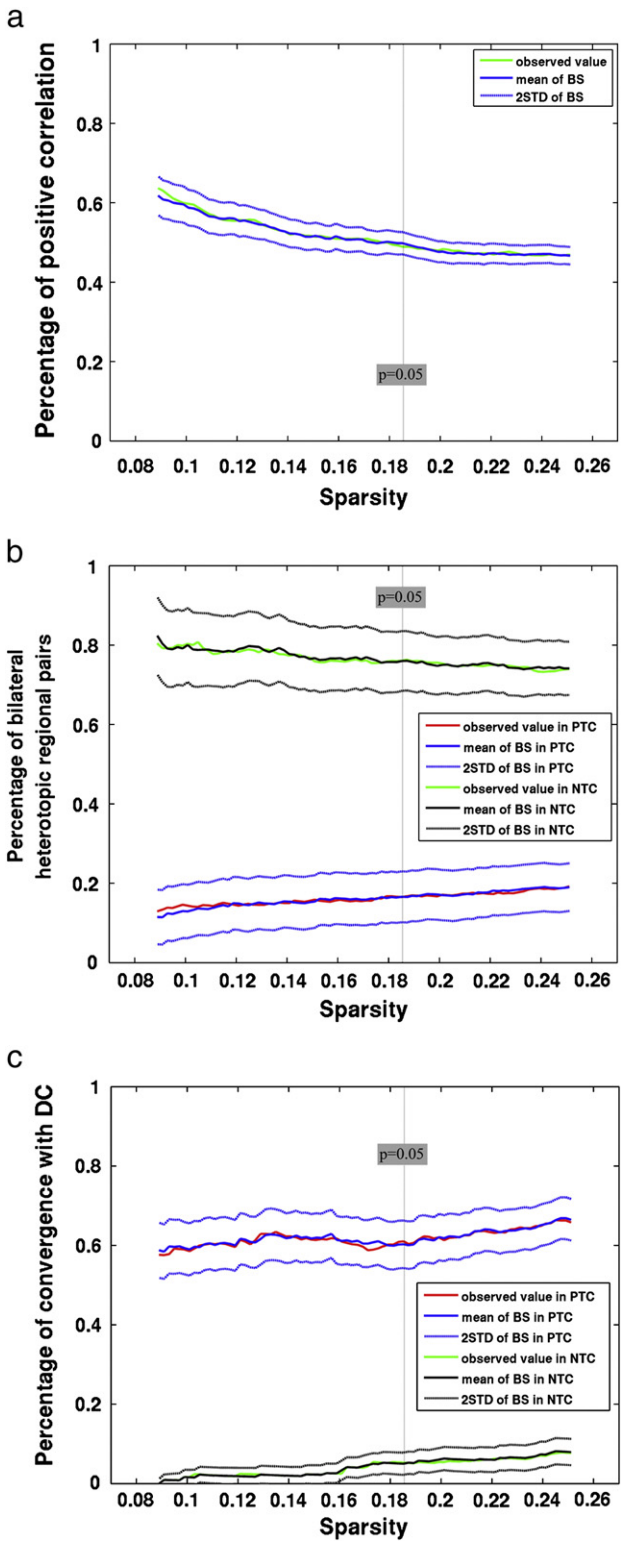

Fig. 5. Statistics-of-interest as a function of sparsity. (a) Percentage of positive thickness correlation relative to all thickness correlations. There is no dramatic disproportion between positive thickness correlation (PTC) and negative thickness correlation (NTC) over the range of sparsity. (b) Percentage of bilateral heterotopic regional pairs in PTC and NTC, respectively. As shown, majority (~80%) of NTC are between bilateral heterotopic regions, while PTC mostly (>80%) links ipsilateral or bilateral homotopic regions. (c) Percentage of PTC and NTC convergent with diffusion connections (DC), respectively. Strikingly, almost all NTC (>90%) are divergent with DC across the entire range of sparsity. The mean and STD of all these statistics were estimated from the 1000 bootstrap samples (BS). The uncorrected $p = 0.05$ for the thickness correlation was marked out (i.e. sparsity of 18.6%). Again, the observed values from the raw 95 subjects (green line) are very close to the mean of BS for all the statistics.

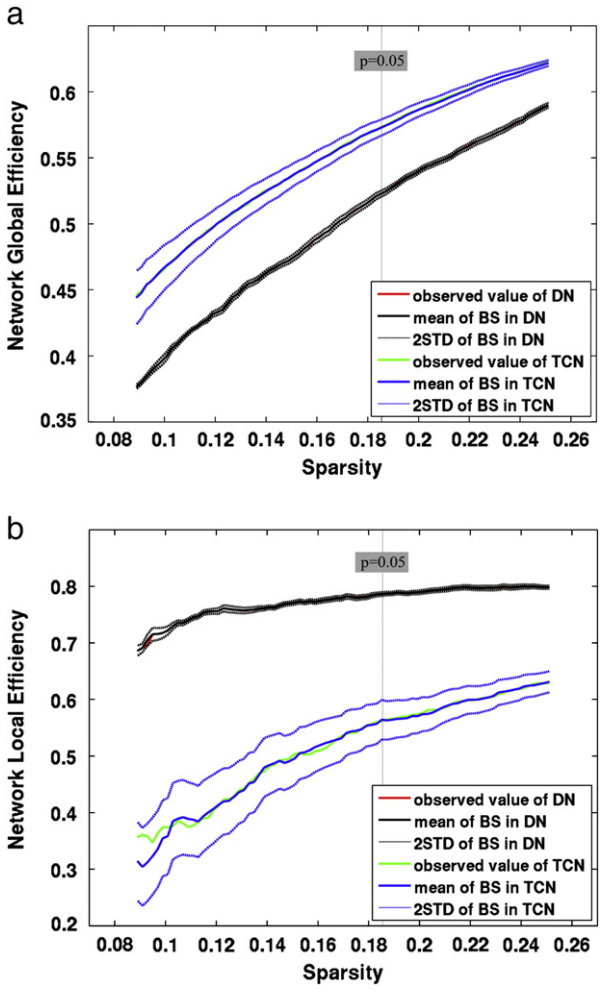

Fig. 6. The comparison of network efficiency between thickness correlation network (TCN) and diffusion networks (DN). (a) The global efficiency of both networks as a function of sparsity; (b) The local efficiency of both networks as a function of sparsity. The uncorrected $p = 0.05$ for the thickness correlation was marked out (i.e. sparsity of 18.6%). The mean and STD of both global and local efficiency for both networks were estimated from the 1000 bootstrap samples (BS). Likewise, the observed values from the raw 95 subjects are very close to the mean of BS. Clearly, the global efficiency of TCN is significantly higher (the maximum $p = 10^{-100}$), but the local efficiency is significantly lower than DN over the entire range of sparsity (the maximum $p = 10^{-100}$).

of sparsity (paired *t*-test: the maximum $p = 10^{-100}$ for local efficiency, and the maximum $p = 10^{-100}$ for global efficiency). Consequently, the integrated local and global efficiencies also showed significant differences between TCN and DN (paired *t*-test: $p = 10^{-100}$). It should be noted that above comparative results between the group DN and TCN capture well the patterns of convergence and divergence between individual DN and the TCN (Fig. 7).

The regional efficiency of each node quantifies its connectivity to all other nodes of the network and therefore high regional efficiency implies a hub role for that node in the network. Here, we specifically reported the results of the integrated E_{reg} over the sparsity range for each node. As done previously (Gong et al., 2009b), regions were identified as the hubs in both cortical networks if their integrated E_{reg} were at least one standard deviation (STD) greater than the average E_{reg} of the network (Table 1 and Fig. 8; for all cortical regions, see Supplementary Table 3.). While there are significant differences in hub regions between these two modal networks, left precuneus and superior parietal gyrus are identified as hub regions in both networks. Notably, the majority of the hub regions in both networks belong to association cortex (Table 1 and Fig. 8). Despite the difference of hub

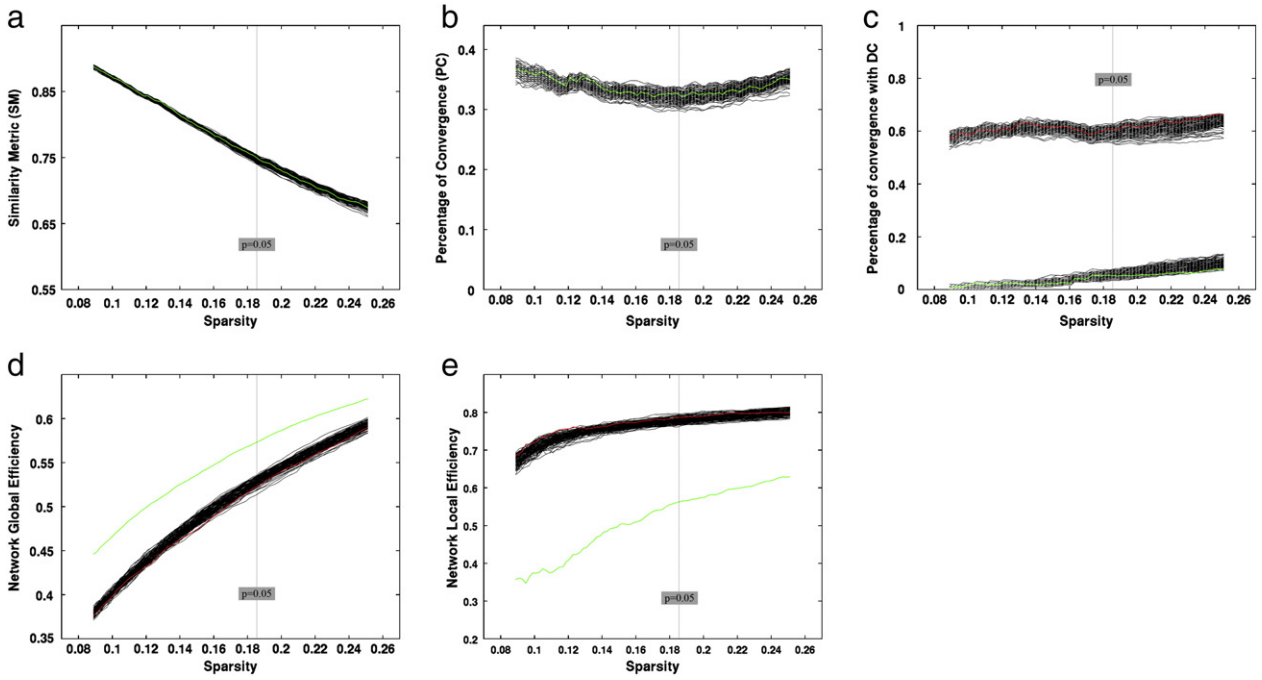

Fig. 7. The comparison between individual DN and TCN. (a) Similarity metric (SM) and (b) Percentage of convergence (PC) between individual DN and TCN as a function of sparsity. Each black line indicates one individual DN, and the green line represents the group-averaged DN. (c) Percentage of convergence with diffusion connections for positive and negative thickness correlations, where individual DN was indicated by black lines and the group-averaged DN was indicated by the red and green line, respectively. (d) Comparison of global efficiency and (e) local efficiency for individual DN (indicated by black lines) and the group-averaged DN (indicated by the red lines), where the green line represents the network efficiency of TCN. Evidently, the comparative results between the group-averaged DN and TCN capture well the patterns of convergence and divergence between individual DN and the TCN.

regions in both networks, the integrated regional efficiencies across all nodes showed statistically significant positive correlation ($R = 0.4$, $p = 0.0006$) between these two modalities, as demonstrated in Fig. 9, suggesting an intrinsic similarity of network topology. The same procedure has been applied to the nodal local efficiency but no significant correlation ($R = -0.11$, $p = 0.32$) was found between the two networks.

Discussion

In this study, cortical thickness correlation and diffusion connectivity based on tractography have been compared quantitatively in the same population. A markedly different pattern of concordance with the diffusion connectivity was observed for positive thickness correlation as compared with negative thickness correlation. Furthermore, using graph theoretic approaches, we found that the TCN has a more randomized overall topology as compared to the DN, whereas the nodal efficiency of cortical regions is significantly correlated between these two modalities.

Table 1
The cortical hub regions (integrated regional efficiencies (E_{reg}) > mean + STD) for both thickness correlation (TCN) and diffusion network (DN).

Rank (E_{reg})	Hubs inTCN	Class	Hubs in DN	Class
1	SPG.R	Association	PCUN.R	Association
2	PCUN.L	Association	PCUN.L	Association
3	SOG.R	Association	PCG.R	Paralimbic
4	MOG.R	Association	INS.L	Paralimbic
5	CUN.R	Association	SFGdor.L	Association
6	DCG.L	Paralimbic	DCG.R	Paralimbic
7	SFGmed.L	Association	ACG.R	Association
8	SPG.L	Association	SPG.L	Association
9	ITG.R	Association	CAL.R	Primary
10	FFG.L	Association	ORBsup.L	Paralimbic
11	ITG.L	Association	OLF.R	Association
12	PCR.R	Association		

The cortical regions were ranked in the order of descending integrated E_{reg} for both cortical networks. L and R represent left and right, respectively. These hub regions have also been displayed on the cortical surface (Fig. 8). As shown, left precuneus (PUN) and superior parietal gyrus (SPG) have high regional efficiency in both modalities. In addition, the majority of these hub regions in both networks consistently belong to association cortex. For the integrated E_{reg} of all nodes, please see Supplementary Table 3.

Thickness correlations vs diffusion connections

Cortical thickness is influenced by multiple factors, including the number, size and myelination of neurons in the cortical columns (Panizzon et al., 2009; Rakic, 1988). The covariance of thickness among various cortical areas thus indicates a synchronization in changes of the local morphology among these areas. So far, the biological cause behind this phenomenon remains undefined. It has been speculated that various brain areas covary as a result of mutually trophic effects that are mediated by direct underlying axonal connections. For instance, neuronal survival and dendritic volume could be promoted in the adult brain by neurotrophic factors such as BDNF and glutamatergic signaling via the NMDA receptor (Burgoyne et al., 1993; Monfils et al., 2004). This trophic theory implies convergence between thickness correlation and diffusion connection among areas. In accordance, thickness correlations among fiber-connected regions have been observed. For instance, most bilateral homotopic regional pairs that are fiber-connected via the corpus callosum have shown significant thickness correlations (He et al., 2007), a feature that is also observed in our present study. Previous optimized voxel-based morphometry (VBM) studies also demonstrated correlation of gray matter density between bilateral homotopic regions (Mechelli et al., 2005). Specifically, Lerch et al. (2006 reported that the pattern of thickness correlation seeding from left inferior frontal area (i.e. Brodmman area 44) is similar to the tractography map of the arcuate fasciculus. However, our data showed that only 35–40% of all regional pairs have convergent thickness correlation and diffusion connection (Fig. 2b).

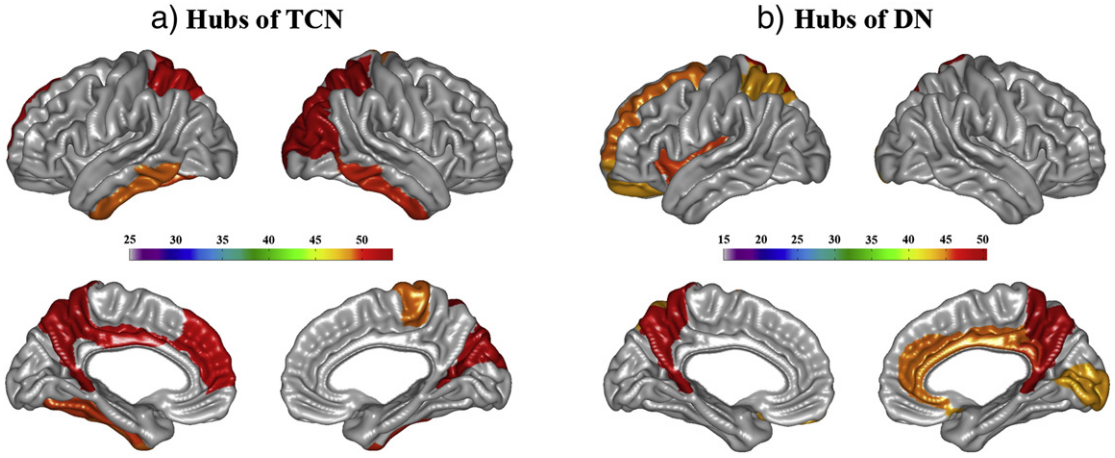

Fig. 8. The hub regions for both TCN (a) and DN (b). Only hub regions (Table 1) are marked on the cortical surface map. The color indicates the integrated regional efficiency (E_{reg}).

As expected, our data demonstrated a degree of agreement between thickness correlation and diffusion connection that is higher than expected by chance (Fig. 2a). However, the substantial proportion of divergence (more than 60%) indicates that thickness correlation cannot be simply considered as a proxy measure for diffusion connection. There must be other factors as well underlying interregional thickness correlation. One possibility is that thickness correlation among areas may be driven by functional associations/connectivity. The coherence of neuronal activity in response to specific functional demands might induce synchronized plastic changes among related regions. For example, previous study has reported that related components of the visual system (i.e., optic tract, lateral geniculate nucleus, and primary visual cortex) covary in volume across individuals (Andrews et al., 1997). Notably, inter-regional functional connection does not necessarily predict underlying direct diffusion connections between regions. It has been frequently observed among cortical regions that can only be indirectly anatomically connected (Honey et al., 2009, 2010). We therefore speculate that the observed thickness correlations that are divergent with diffusion connection may reflect functional connections that have no direct anatomical connection. However, this speculation is complicated by the fact that the AAL-defined regions in the present study may be functionally inhomogeneous. Specific study should be conducted in the future to test this hypothesis by comparing morphometric networks with functional networks in the same population. Finally, we cannot rule out the possibility that thickness correlation is driven by neither anatomical nor functional connections, but instead is determined by genetic effects (Schmitt et al., 2008) or similarities in tissue type (Cohen et al., 2008).

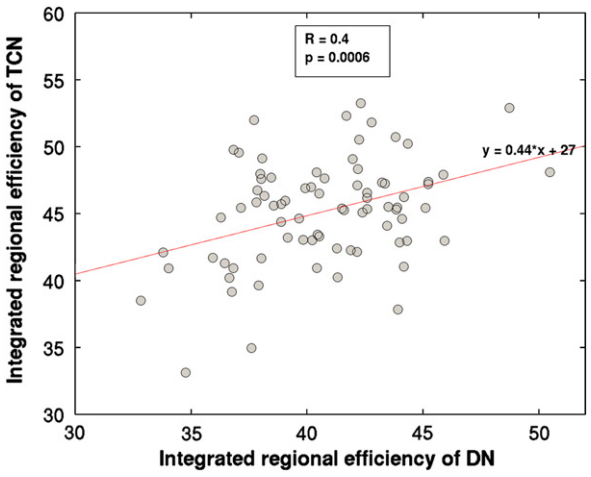

Fig. 9. The significant correlation of integrated regional efficiency between thickness correlation (TCN) and diffusion networks (DN). Each circle represents one AAL region.

Intriguingly, the observed convergences between thickness correlation and diffusion connection are overwhelmingly focused on the positive correlations (Fig. 5c). This is compatible with the hypothesis of trophic effect via direct axonal connections, which theoretically should result in thickness changes in the same direction, therefore leading to positive correlations between related regions. On the other hand, the dramatic divergence of negative thickness correlation from diffusion connections suggests negative thickness correlation may be a reflection of functional connectivity between antagonistic areas. Previous studies have consistently observed negative functional connectivity between areas by using functional MRI techniques. For example, negative correlations between regions placed within the default network and regions within the dorsal attention system were repeatedly reported at the group level (Fox et al., 2005). The observed negative correlation implies that brain systems are functionally in competition with one another. However, the interpretation of negative correlation requires caution, given the fact that data-processing such as global signal removal can artificially induce negative correlations (Van Dijk et al., 2010). Furthermore, we found that the majority of negative correlations of thickness (around 80%, Fig. 5b) are between bilateral heterotopic regions, while positive ones mainly link ipsilateral or bilateral homotopic regions. This pattern of thickness correlation is consistent with previous observations showing negative associations of gray matter density largely between bilateral heterotopic regions (Mechelli et al., 2005).

Topological relation between the TCN and DN

The cerebral cortex was further characterized as a complex network in which each AAL region represents a network node and two nodes/areas are considered linked if they are statistically correlated in cortical thickness (i.e. TCN) or are anatomically connected (i.e. DN). The TCN and DN capture the underlying organization of structural association and fiber connection of the cerebral cortex, respectively. Graph theoretical analysis provides a powerful mathematical framework for characterizing topological properties of the complex graphs/networks and is being translated to explore human brain networks derived from multi-modal neuroimaging data (Bullmore and Sporns, 2009; He and Evans, 2010). Using graph theoretical analysis, a small-world topology has been consistently observed across multi-modal brain networks (morphometric correlation, diffusion and functional networks) in previous studies (Achard et al., 2006; Gong et al., 2009b; He et al., 2007). The small-world model theoretically supports both specialized/modularized and integrated/distributed information

processing and maximizes the efficiency of information transfer both globally and locally at a relatively low wiring cost. In the present study, although both cortical networks are within the small-world regime, the global and local efficiencies between the two networks are significantly different (Fig. 6). While topological differences between these two modal networks are expected due to the observed divergence of thickness correlation with diffusion connection, the pattern of the topological difference should be noted. Specifically, the TCN has a significantly higher global efficiency but a much lower local efficiency than the DN over the entire range of sparsity, which suggests a more randomized and less modularized topology of the TCN. This possibly relates to the combined effect of the multiple factors behind cortical thickness correlation, giving rise to more long-range paths and a more random configuration.

In addition to the overall network parameters, the regional efficiency was calculated for each node in both cortical networks. This parameter measures a node's connectivity to all other nodes of the network and quantifies the importance of a node for the information transfer within the network. High regional efficiency implies a hub/-core role for that node (Achard et al., 2006). In our data, we found that there are significant differences in hub regions for the two modal networks (Table 1 and Fig. 8), but the majority of the hub regions in both networks consistently belonged to association cortex that plays a central role receiving inputs from multiple cortical regions (Mesulam, 2000). This is consistent with the findings that cortical hubs revealed by intrinsic functional connectivity are located throughout heteromodal areas of association cortex (Achard et al., 2006). Notably, left precuneus and superior parietal gyrus were identified as hub regions in both networks, consistent with recent findings showing a structural core within posterior medial and parietal cortex (Hagmann et al., 2008). Despite the difference of hub regions between thickness correlation and diffusion networks, the regional efficiencies across all nodes showed statistically significant concordance between these two modalities (Fig. 9), suggesting an intrinsic similarity of information traffic patterns in both networks. This is compatible with previous findings that show highly correlated regional centrality between structural and functional networks using computational approaches (Honey et al., 2007). In addition, a recent study has reported significant covariations between the regional efficiency of diffusion connectivity network and regional cerebral blood flow measured by perfusion MRI (Várkuti et al., 2011), suggesting a potential role of regional metabolism to the correlation of nodal efficiency between the two modalities in the present study.

Methodological issues

Several methodological issues need to be addressed. First, while diffusion MRI tractography has been widely employed to reconstruct specific WM tracts among regions-of-interest, it remains imperfect to map out all the connections accurately throughout the entire brain. For example, current tractography algorithms may show biases against long distance connections, which may result in the loss of some long-range connections. In addition, diffusion tractography remains a limited capacity for resolving crossing fiber bundles, accounting for the missing of other existing connections, e.g. between the lateral inter-hemispheric regions. Therefore, it is important to note that while the overall connectivity pattern has been largely captured by the diffusion network, it has been noised to some degree, containing both false negative (i.e. missed connections) and false positive connections (i.e. spurious connections) even after the thresholding procedure. Future studies with more sophisticated tractography algorithms or diffusion imaging techniques, as well as finer imaging resolution or quality, need to be conducted to yield a more accurate representation of the underlying brain anatomical networks. Second, we measured the thickness correlations between cortical regions by using Pearson full correlation. There are alternative choices such as partial correlation, estimating the pairwise association between any two brain regions while controlling for the effects of the other brain regions. The comparison between diffusion connections and thickness partial correlations needs to be addressed in the future. Third, we confined the analysis to the cerebral cortical system in the current study, given the fact that the morphometric descriptor (thickness) can only be defined within the cerebral cortex. The sub-cortical structures such as the striatum and thalamus play important roles on the cortical dynamics and will be included in the future, e.g. when exploring other morphometric descriptors such as volume. Finally, the thickness correlations and diffusion connections are extracted between cortical regions that are obtained from a prior atlas (AAL template). There exist alternative strategies for the cortical parcellation by using other templates, like Brodmman atlas. It has been demonstrated that brain network topology depends on the scheme of brain parcellation (Wang et al., 2009; Zalesky et al., 2010). Future studies could be conducted to test the effect of cortical parcellation on the relation between the two measures.

Conclusion

Our study revealed both substantial convergence and divergence between cortical thickness correlation and diffusion connection across the human cerebral cortex. Intriguingly, the agreement of positive and negative thickness correlations with diffusion connections is quite different, suggesting that different mechanisms underlie the direction of thickness correlation. Moreover, our study showed that the thickness correlation network has a more randomized overall topology than the diffusion network, whereas the nodal characteristics of cortical regions in these two networks are statistically correlated. Our findings indicate that thickness correlation contains exclusive information representing an important aspect of interregional association/interaction, and therefore should not be simply taken as a proxy measure for diffusion connection. The interregional correlations of other morphometric descriptors such as gray matter volume and cortical area have also been used to study brain connectivity, which putatively characterize distinct properties of the interaction or different aspects of the same interaction (mechanical, anatomical, and chemical) between brain structures (Sanabria-Diaz et al., 2010). It would be intriguing in future to explore how the interregional correlation of different morphometric descriptors, anatomical connection and functional connection are related to each other, by combining structural MRI, diffusion MRI and functional MRI for the same population.

Acknowledgments

This work was conducted as part of the International Consortium for Brain Mapping (ICBM), funded by the consortium grant NIH9-P01EB001955-11 (PI, John Mazziotta, UCLA). G. G. was supported by the Canadian Imperial Bank of Commerce (CIBC) brain imaging fellowship of the Montreal Neurological Institute and Hospital.

Appendix A. Supplementary data

Supplementary data to this article can be found online at doi:10.1016/j.neuroimage.2011.08.017.

References

Achard, S., Bullmore, E., 2007. Efficiency and cost of economical brain functional networks. PLoS Comput Biol. 3, e17.
Achard, S., Salvador, R., Whitcher, B., Suckling, J., Bullmore, E., 2006. A resilient, low-frequency, small-world human brain functional network with highly connected association cortical hubs. J. Neurosci. 26, 63–72.
Andrews, T.J., Halpern, S.D., Purves, D., 1997. Correlated size variations in human visual cortex, lateral geniculate nucleus, and optic tract. J. Neurosci. 17, 2859–2868.

Bassett, D.S., Bullmore, E., Verchinski, B.A., Mattay, V.S., Weinberger, D.R., Meyer-Lindenberg, A., 2008. Hierarchical organization of human cortical networks in health and schizophrenia. J. Neurosci. 28, 9239–9248.
Behrens, T.E., Johansen-Berg, H., Woolrich, M.W., Smith, S.M., Wheeler-Kingshott, C.A., Boulby, P.A., Barker, G.J., Sillery, E.L., Sheehan, K., Ciccarelli, O., Thompson, A.J., Brady, J.M., Matthews, P.M., 2003a. Non-invasive mapping of connections between human thalamus and cortex using diffusion imaging. Nat. Neurosci. 6, 750–757.
Behrens, T.E., Woolrich, M.W., Jenkinson, M., Johansen-Berg, H., Nunes, R.G., Clare, S., Matthews, P.M., Brady, J.M., Smith, S.M., 2003b. Characterization and propagation of uncertainty in diffusion-weighted MR imaging. Magn. Reson. Med. 50, 1077–1088.
Behrens, T.E., Berg, H.J., Jbabdi, S., Rushworth, M.F., Woolrich, M.W., 2007. Probabilistic diffusion tractography with multiple fibre orientations: what can we gain? NeuroImage 34, 144–155.
Bullmore, E., Sporns, O., 2009. Complex brain networks: graph theoretical analysis of structural and functional systems. Nat. Rev. Neurosci. 10, 186–198.
Burgoyne, R.D., Graham, M.E., Cambraydeakin, M., 1993. Neurotrophic effects of NMDA receptor activation on developing cerebellar granule cells. J. Neurocytol. 22, 689–695.
Chen, Z.J., He, Y., Rosa-Neto, P., Germann, J., Evans, A.C., 2008. Revealing modular architecture of human brain structural networks by using cortical thickness from MRI. Cereb. Cortex. 18, 2374–2381.
Cohen, M.X., Lombardo, M.V., Blumenfeld, R.S., 2008. Covariance-based subdivision of the human striatum using T1-weighted MRI. Eur. J. Neurosci. 27, 1534–1546.
Collins, D.L., Neelin, P., Peters, T.M., Evans, A.C., 1994. Automatic 3D intersubject registration of MR volumetric data in standardized Talairach space. J. Comput. Assist. Tomogr. 18, 192–205.
Dijkstra, E.W., 1959. A note on two problems in connexion with graphs. Numer. Math. 1, 269–271.
Efron, B., Tibshirani, R., 1993. An Introduction to the Bootstrap, xvi. Chapman & Hall, New York. 436 p. p.
Ferrer, I., Blanco, R., Carulla, M., Condom, M., Alcantara, S., Olive, M., Planas, A., 1995. Transforming growth factor-alpha immunoreactivity in the developing and adult brain. Neuroscience 66, 189–199.
Fox, M.D., Snyder, A.Z., Vincent, J.L., Corbetta, M., Van Essen, D.C., Raichle, M.E., 2005. The human brain is intrinsically organized into dynamic, anticorrelated functional networks. Proc. Natl. Acad. Sci. U. S. A. 102, 9673–9678.
Gong, G., He, Y., Concha, L., Lebel, C., Gross, D.W., Evans, A.C., Beaulieu, C., 2009a. Mapping anatomical connectivity patterns of human cerebral cortex using in vivo diffusion tensor imaging tractography. Cereb. Cortex. 19, 524–536.
Gong, G., Rosa-Neto, P., Carbonell, F., Chen, Z.J., He, Y., Evans, A.C., 2009b. Age- and gender-related differences in the cortical anatomical network. J. Neurosci. 29, 15684–15693.
Hagmann, P., Cammoun, L., Gigandet, X., Meuli, R., Honey, C.J., Wedeen, V.J., Sporns, O., 2008. Mapping the structural core of human cerebral cortex. PLoS Biol. 6, e159.
He, Y., Evans, A., 2010. Graph theoretical modeling of brain connectivity. Curr. Opin. Neurol. 23, 341–350.
He, Y., Chen, Z.J., Evans, A.C., 2007. Small-world anatomical networks in the human brain revealed by cortical thickness from MRI. Cereb. Cortex. 17, 2407–2419.
He, Y., Chen, Z., Evans, A., 2008. Structural insights into aberrant topological patterns of large-scale cortical networks in Alzheimer's disease. J. Neurosci. 28, 4756–4766.
He, Y., Dagher, A., Chen, Z., Charil, A., Zijdenbos, A., Worsley, K., Evans, A., 2009. Impaired small-world efficiency in structural cortical networks in multiple sclerosis associated with white matter lesion load. Brain 132, 3366–3379.
Honey, C.J., Kotter, R., Breakspear, M., Sporns, O., 2007. Network structure of cerebral cortex shapes functional connectivity on multiple time scales. Proc. Natl. Acad. Sci. U. S. A. 104, 10240–10245.
Honey, C.J., Sporns, O., Cammoun, L., Gigandet, X., Thiran, J.P., Meuli, R., Hagmann, P., 2009. Predicting human resting-state functional connectivity from structural connectivity. Proc. Natl. Acad. Sci. U. S. A. 106, 2035–2040.
Honey, C.J., Thivierge, J.P., Sporns, O., 2010. Can structure predict function in the human brain? NeuroImage 52, 766–776.
Iturria-Medina, Y., Sotero, R.C., Canales-Rodriguez, E.J., Aleman-Gomez, Y., Melie-Garcia, L., 2008. Studying the human brain anatomical network via diffusion-weighted MRI and Graph Theory. NeuroImage 40, 1064–1076.
Kabani, N., Le Goualher, G., MacDonald, D., Evans, A.C., 2001. Measurement of cortical thickness using an automated 3-D algorithm: a validation study. NeuroImage 13, 375–380.
Kim, J.S., Singh, V., Lee, J.K., Lerch, J., Ad-Dab'bagh, Y., MacDonald, D., Lee, J.M., Kim, S.I., Evans, A.C., 2005. Automated 3-D extraction and evaluation of the inner and outer cortical surfaces using a Laplacian map and partial volume effect classification. NeuroImage 27, 210–221.
Latora, V., Marchiori, M., 2003. Economic small-world behavior in weighted networks. Eur. Phys. J. B. 32, 249–263.
Lee, J.K., Lee, J.M., Kim, J.S., Kim, I.Y., Evans, A.C., Kim, S.I., 2006. A novel quantitative cross-validation of different cortical surface reconstruction algorithms using MRI phantom. NeuroImage 31, 572–584.
Lerch, J.P., Evans, A.C., 2005. Cortical thickness analysis examined through power analysis and a population simulation. NeuroImage 24, 163–173.
Lerch, J.P., Worsley, K., Shaw, W.P., Greenstein, D.K., Lenroot, R.K., Giedd, J., Evans, A.C., 2006. Mapping anatomical correlations across cerebral cortex (MACACC) using cortical thickness from MRI. NeuroImage 31, 993–1003.
Li, S., Han, Y., Wang, D., Yang, H., Fan, Y., Lv, Y., Tang, H., Gong, Q., Zang, Y., He, Y., 2010. Mapping surface variability of the central sulcus in musicians. Cereb. Cortex. 20, 25–33.
Lo, C.Y., Wang, P.N., Chou, K.H., Wang, J., He, Y., Lin, C.P., 2010. Diffusion tensor tractography reveals abnormal topological organization in structural cortical networks in Alzheimer's disease. J. Neurosci. 30, 16876–16885.
Luce, R.D., Perry, A.D., 1949. A method of matrix analysis of group structure. Psychometrika 14 (1), 95–116.
MacDonald, D., Kabani, N., Avis, D., Evans, A.C., 2000. Automated 3-D extraction of inner and outer surfaces of cerebral cortex from MRI. NeuroImage 12, 340–356.
Maslov, S., Sneppen, K., 2002. Specificity and stability in topology of protein networks. Science 296, 910–913.
Mechelli, A., Friston, K.J., Frackowiak, R.S., Price, C.J., 2005. Structural covariance in the human cortex. J. Neurosci. 25, 8303–8310.
Mesulam, M.M., 2000. Principles of behavioral and cognitive neurology, xviii. Oxford University Press, Oxford; New York. 540 p. p.
Monfils, M.H., VandenBerg, P.M., Kleim, J.A., Teskey, G.C., 2004. Long-term potentiation induces expanded movement representations and dendritic hypertrophy in layer V of rat sensorimotor neocortex. Cereb. Cortex. 14, 586–593.
Panizzon, M.S., Fennema-Notestine, C., Eyler, L.T., Jernigan, T.L., Prom-Wormley, E., Neale, M., Jacobson, K., Lyons, M.J., Grant, M.D., Franz, C.E., Xian, H., Tsuang, M., Fischl, B., Seidman, L., Dale, A., Kremen, W.S., 2009. Distinct genetic influences on cortical surface area and cortical thickness. Cereb. Cortex. 19, 2728–2735.
Rakic, P., 1988. Specification of cerebral cortical areas. Science 241, 170–176.
Sanabria-Diaz, G., Melie-Garcia, L., Iturria-Medina, Y., Aleman-Gomez, Y., Hernandez-Gonzalez, G., Valdes-Urrutia, L., Galan, L., Valdes-Sosa, P., 2010. Surface area and cortical thickness descriptors reveal different attributes of the structural human brain networks. NeuroImage 50, 1497–1510.
Schmitt, J.E., Lenroot, R.K., Wallace, G.L., Ordaz, S., Taylor, K.N., Kabani, N., Greenstein, D., Lerch, J.P., Kendler, K.S., Neale, M.C., Giedd, J.N., 2008. Identification of genetically mediated cortical networks: a multivariate study of pediatric twins and siblings. Cereb. Cortex. 18, 1737–1747.
Sled, J.G., Zijdenbos, A.P., Evans, A.C., 1998. A nonparametric method for automatic correction of intensity nonuniformity in MRI data. IEEE Trans. Med. Imaging 17, 87–97.
Thompson, P.M., Schwartz, C., Lin, R.T., Khan, A.A., Toga, A.W., 1996. Three-dimensional statistical analysis of sulcal variability in the human brain. J. Neurosci. 16, 4261–4274.
Tohka, J., Zijdenbos, A., Evans, A., 2004. Fast and robust parameter estimation for statistical partial volume models in brain MRI. NeuroImage 23, 84–97.
Tzourio-Mazoyer, N., Landeau, B., Papathanassiou, D., Crivello, F., Etard, O., Delcroix, N., Mazoyer, B., Joliot, M., 2002. Automated anatomical labeling of activations in SPM using a macroscopic anatomical parcellation of the MNI MRI single-subject brain. NeuroImage 15, 273–289.
Van Dijk, K.R., Hedden, T., Venkataraman, A., Evans, K.C., Lazar, S.W., Buckner, R.L., 2010. Intrinsic functional connectivity as a tool for human connectomics: theory, properties, and optimization. J. Neurophysiol. 103, 297–321.
Várkuti, B., Cavusoglu, M., Kullik, A., Schiffler, B., Veit, R., Yilmaz, Ö., Rosenstiel, W., Braun, C., Uludag, K., Birbaumer, N., Sitaram, R., 2011. Quantifying the link between anatomical connectivity, gray matter volume and regional cerebral blood flow: an integrative MRI study. PLoS ONE 6, e14801.
Wang, J., Wang, L., Zang, Y., Yang, H., Tang, H., Gong, Q., Chen, Z., Zhu, C., He, Y., 2009. Parcellation-dependent small-world brain functional networks: a resting-state fMRI study. Hum. Brain Mapp. 30, 1511–1523.
Watts, D.J., Strogatz, S.H., 1998. Collective dynamics of 'small-world' networks. Nature 393, 440–442.
Wen, W., Zhu, W., He, Y., Kochan, N.A., Reppermund, S., Slavin, M.J., Brodaty, H., Crawford, J., Xia, A., Sachdev, P., 2011. Discrete neuroanatomical networks are associated with specific cognitive abilities in old age. J. Neurosci. 31, 1204–1212.
Zalesky, A., Fornito, A., Harding, I.H., Cocchi, L., Yucel, M., Pantelis, C., Bullmore, E.T., 2010. Whole-brain anatomical networks: does the choice of nodes matter? NeuroImage 50, 970–983.
Zijdenbos, A.P., Forghani, R., Evans, A.C., 2002. Automatic "pipeline" analysis of 3-D MRI data for clinical trials: application to multiple sclerosis. IEEE Trans. Med. Imaging 21, 1280–1291.
Zilles, K., Schleicher, A., Langemann, C., Amunts, K., Morosan, P., Palomero-Gallagher, N., Schormann, T., Mohlberg, H., Burgel, U., Steinmetz, H., Schlaug, G., Roland, P.E., 1997. Quantitative analysis of sulci in the human cerebral cortex: development, regional heterogeneity, gender difference, asymmetry, intersubject variability and cortical architecture. Hum. Brain Mapp. 5, 218–221.